Design of Narrow-Gap TiO_2: A Passivated Codoping Approach for Enhanced Photoelectrochemical Activity

Yanqin Gai,[1] Jingbo Li,[1,*] Shu-Shen Li,[1] Jian-Bai Xia,[1] and Su-Huai Wei[2,†]

[1]*State Key Laboratory for Superlattices and Microstructures, Institute of Semiconductors, Chinese Academy of Sciences, P.O. Box 912, Beijing 100083, China*

[2]*National Renewable Energy Laboratory, Golden, Colorado 80401, USA*

(Received 31 October 2008; published 20 January 2009)

To improve the photoelectrochemical activity of TiO_2 for hydrogen production through water splitting, the band edges of TiO_2 should be tailored to match with visible light absorption and the hydrogen or oxygen production levels. By analyzing the band structure of TiO_2 and the chemical potentials of the dopants, we propose that the band edges of TiO_2 can be modified by passivated codopants such as (Mo + C) to shift the valence band edge up significantly, while leaving the conduction band edge almost unchanged, thus satisfying the stringent requirements. The design principle for the band-edge modification should be applicable to other wide-band-gap semiconductors.

DOI: 10.1103/PhysRevLett.102.036402 PACS numbers: 71.20.Nr, 61.72.Bb, 61.72.up, 71.55.Ht

TiO_2 has strong catalytic activity, high chemical stability, and a long lifetime of photon-generated carriers, making it one of the most promising photocatalysts for hydrogen production through photoelectrochemical (PEC) water splitting and for other applications such as water or air purification and dye-sensitized solar cells [1–4]. The water-splitting process [1,2], as shown in Fig. 1, utilizes both the reducing and oxidation powers of TiO_2. The reducing power is measured by the conduction band minimum (CBM) energy. The closer the CBM energy to the vacuum level, the stronger the reducing power is. On the other hand, the oxidizing power is measured by the valence band maximum (VBM) energy. The lower the VBM energy, the higher the oxidizing power. For a spontaneous PEC water-splitting process, the oxygen and hydrogen reactions must lie between the VBM and CBM; i.e., the band edges must straddle the water redox potential levels. The band alignments of TiO_2 satisfy this requirement with a CBM energy slightly above the hydrogen production level and VBM far below the water oxidation level (see Fig. 1). However, the energy conversion efficiency of TiO_2 is low. This is mainly because TiO_2 has a wide band gap of about 3.2 eV; thus, TiO_2 absorbs only a small portion of the solar spectrum in the ultraviolet region. It is well known that to achieve high efficiency, the desirable photocatalyst should have a band gap around 2.0 eV and the positions of its band edges must be matched with the redox potentials of water [5].

In the last few years, great efforts have been made to modify the band structure of TiO_2 to shift its absorption edge toward the visible light region and place its band edges at proper positions, thus improving its photocatalytic efficiency. One way of doing so is to dope TiO_2 with either anions or cations [6–10]. For example, TiO_2 doped with substitutional nitrogen creates an acceptor level above the VBM. The presence of such states has led to an effective band-gap narrowing and some visible-light PEC water-splitting activities. However, experimental studies also show that for this kind of monodoping, photogenerated current is low because the partially occupied impurity bands can act as recombination centers and reduce the photogenerated current. Monodoping with 3*d* transitional metal ions has also been investigated extensively for expanding the photo response of TiO_2 into the visible region. Although this approach was able to reduce the band gap of TiO_2 to some extent, it also suffers from the existence of a carrier recombination center and the formation of strongly localized *d* states within the band gap, which significantly reduce carrier mobility [11–13].

In this Letter, we propose using a passivated codoping approach to redshift the TiO_2 absorption edge and improve its photocatalytic efficiency for hydrogen production. Because the defect bands are passivated, they will not be effective as carrier recombination centers [14,15]. After

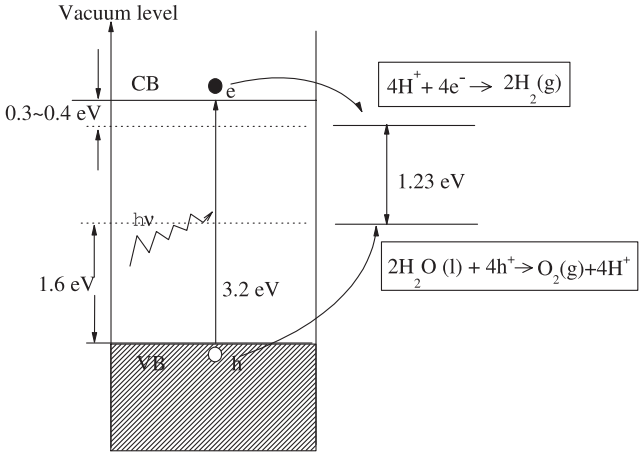

FIG. 1. Position of the band edges of TiO_2 relative to the standard levels of hydrogen production and water oxidation.

analyzing the band structure of TiO_2 and the chemical potentials of the dopants, we suggest that (Mo + C)-doped TiO_2 could be a strong candidate for PEC water splitting, because it does not affect much of the CBM, but increases the VBM edge significantly. This is required, because the CBM of TiO_2 is only slightly higher than the reducing potential of water, but the VBM of TiO_2 is far lower than the oxidizing potential of water (Fig. 1).

The band structure and total energy calculations are performed using the frozen-core projector-augmented-wave (PAW) method [16] within the local density approximation (LDA) as implemented in the VASP codes [17]. The cutoff energy for the plane-wave basis set is 400 eV. TiO_2 can exist in several different phases. Here, we choose anatase TiO_2, because the CBM of this phase is about 0.1 eV higher than that of rutile, which render the former more applicable for hydrogen production [18]. Our calculated lattice parameters for primitive anatase TiO_2 are $a = 3.768$ Å, $c = 9.458$ Å, and $u = 0.208$, which are in good agreement with experimental values [19]. The calculated band gap is 1.874 eV, much smaller than the experimental band gap of 3.2 eV due to the well-known LDA error. However, in this study we focus on the change of the band gap after doping, so we expect the LDA band-gap error is largely canceled between different systems. To simulate doping, a 48-atom $2 \times 2 \times 2$ supercell is employed. For the Brillouin zone integration, a $2 \times 2 \times 2$ Monkhorst-Pack [20] k-point mesh is used; a more refined $8 \times 8 \times 8$ k-point mesh is used for the density-of-states (DOS) plots.

Band-edge characters of TiO_2.—To modify the band structure of TiO_2 through doping, we first need to know the atomic wave function characters of the band-edge states. As can be seen from the total DOS and partial density of states (PDOS) plots for bulk TiO_2 in Fig. 2, the valence band edge of TiO_2 consists mainly of O $2p$ states, whereas the conduction band edge has predominantly Ti d character. Therefore, to modify the valence band edge (p-type doping), we should choose dopants with different atomic p orbital energy than O, whereas to modify the conduction band edge (n-type doping), we should choose dopants with different atomic d orbital energies than Ti.

Monodoping in TiO_2.—In this study, we choose $3d$ transition metals V and Cr, and $4d$ transition metals Nb and Mo substituting on the Ti site as the n-type dopants and N and C substituting on the O site as the p-type dopants. Figure 3 shows the calculated DOS for anion and cation monodoped TiO_2. Here, the DOS in the different systems are aligned by referencing to the core levels of the atom farthest from the impurity. As expected, the incorporation of N or C on oxygen lattice sites induces acceptor states above the VBM of TiO_2. The position of the acceptor level with respect to the VBM, which has mostly O $2p$ character, is largely determined by the anions' $2p$ orbital energies. The neutral $2p$ orbital energy of carbon and nitrogen are 3.8 and 2.0 eV higher, respectively, than O $2p$ orbital energy. Therefore, the acceptor levels induced by C is deep inside the gap of TiO_2 [Fig. 3(b)], whereas the N acceptor level is relatively shallow [Fig. 3(a)] [21]. Also, as carbon has two less valence electrons than oxygen, the substitution of C on the O site acts as a double acceptor. Similarly, substitution of nitrogen on the O site acts as a single acceptor.

When transition metals (TMs) are used to substitute for Ti in TiO_2, the largest perturbation occurs at the CBM, which has mostly Ti d character. The position of the created donor state near the CBM depends on the d orbital energy of the dopants. Our calculations show that V_{Ti} [Fig. 3(c)] and Cr_{Ti} [Fig. 3(d)] creates deep donor levels

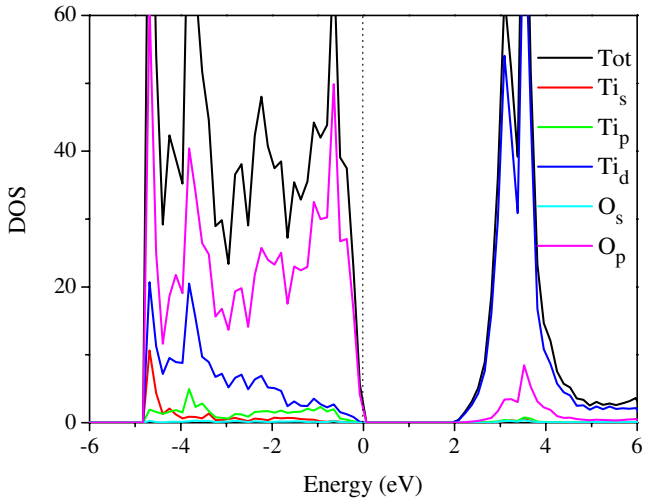

FIG. 2 (color online). The LDA-calculated total and atom-projected DOS of TiO_2. The highest occupied state is chosen as the Fermi energy and is set to zero.

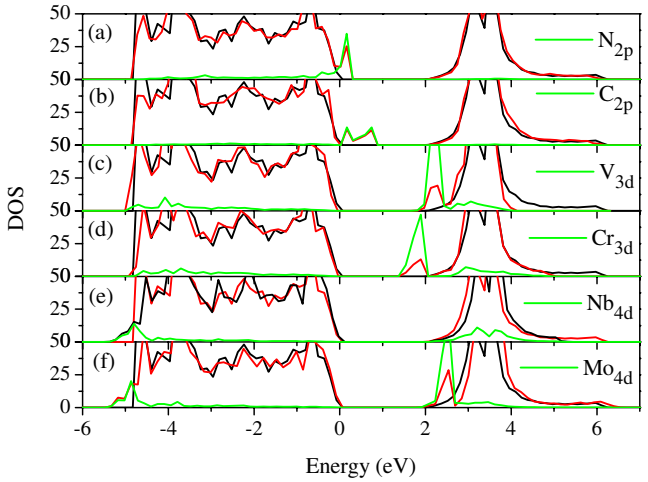

FIG. 3 (color online). The LDA-calculated total DOS for monodoped TiO_2 (red or gray) compared with pure TiO_2 (black) and the partial DOS for impurity atoms (green or light gray). The partial DOS plots are amplified for clarity.

inside the band gap, whereas the defect levels of Nb_{Ti} [Fig. 3(e)] and Mo_{Ti} [Fig. 3(f)] are shallower. To understand this trend, we calculated d orbital eigenvalues of these transition metals in $d^n s^0$ configurations ($n = 2$ for Ti, $n = 3$ for V and Nb, and $n = 4$ for Cr and Mo). We find that with respect to Ti d orbital, the $3d$ orbital energies of V and Cr are 1.8 and 3.3 eV lower than that of Ti $3d$ orbital energy. The $4d$ orbital energy of Mo is 1.2 eV lower, whereas the Nb $4d$ orbital is 0.5 eV *higher* than Ti $3d$ orbital energy. The shallowness of the $4d$ orbital energy compared to the $3d$ is related to the more delocalized character of the $4d$ orbital. The difference between the $3d$ and $4d$ orbital energies will increase further if the ionization state of the TM increases. Therefore, because the $3d$ orbital energy of Cr is the lowest among the TM dopants, the defect level of Cr_{Ti} is the deepest inside the band gap away from the CBM of the host. V_{Ti} donor level is relatively shallower than Cr_{Ti}. The most interesting dopants are Mo and Nb, whose $4d$ orbital energies are close to, or higher than, that of Ti $3d$. When Ti is replaced by Mo or Nb, the defect levels are resonant with the conduction band. Therefore, Mo and Nb are ideal n-type dopants that cause little perturbation at the CBM. For these TM dopants, both V and Nb have one more valence electron than Ti, so they are single donors, whereas Cr and Mo are double donors.

Passivated codoping in TiO_2.—The above-mentioned monodoped systems create partially occupied impurity bands that can facilitate the formation of recombination centers, and thus reduce the PEC efficiency. To avoid this problem, we propose to dope TiO_2 using charge-compensated donor-acceptor pairs such as (N + V), (Nb + N), (Cr + C), and (Mo + C). In these cases, the electrons on the donor levels passivate the same amount of holes on the acceptor levels, so the systems still keep semiconductor character. Figure 4 shows the total DOS of (V + N), (Nb + N), (Cr + C), and (Mo + C)-codoped TiO_2 and compares the results with that for pure TiO_2. We see that the VBM increased greatly compared to the pure TiO_2, whereas the change of CBM is small. Table I lists the shifts of the band edges and changes of the band gaps that are due to the formation of impurity bands from passivated donor and acceptor pairs with respect to that of pure TiO_2.

We can see that the band-edge shifts caused by the donor-acceptor passivated codoping follow the same chemical trends as that observed in the corresponding monodoped cases. Because both single acceptor N_O and single donor V_{Ti} are relatively shallow impurities, (N + V) codoping in TiO_2 reduces the band gap by only 0.49 eV. This is also the case for (Nb + N) codoping, as Nb_{Ti} creates a resonant donor state inside the conduction band. The (Cr + C) codoped system has a much smaller band gap than that of TiO_2, which can be accounted for by the relatively deep double donor Cr_{Ti} and double acceptor C_O levels. However, as discussed above, to improve the PEC efficiency of TiO_2 for water splitting, not only do we need to reduce its band gap to match the visible-light region, we also need to adjust the band-edge energy levels to maintain the redox power of TiO_2. As shown in Fig. 1, this means that we should keep the CBM energy of the modified TiO_2 as high as possible to utilize the reducing power of TiO_2. In view of this requirement, TiO_2 with (Cr + C) codoping is not suitable for H_2 production, as the conduction band edge moved downwards by more than 0.3 eV compared with the pure TiO_2 [Fig. 4(c)]. In the case of conduction band-edge matching, (Nb + N) codoping would be a better choice as it upshifts the CBM toward the vacuum level. However, the effect of (Nb + N) on the band-gap narrowing is too small: the band-gap reduction is less than 0.4 eV. We find that among all the systems, TiO_2:(Mo + C) has the highest figure of merit for PEC water splitting, because not only does it reduce the band gap by about 1.1 eV, ideal for absorbing visible light, it also causes very small perturbation on the position of the conduction band edge as shown in Fig. 4(d). This is because Mo introduces only a shallow donor level below the CBM [Fig. 3(f)], and the coupling to C makes its energy even higher. Therefore, unlike the Cr-doped case, we expect that the (Mo + C)-codoped TiO_2

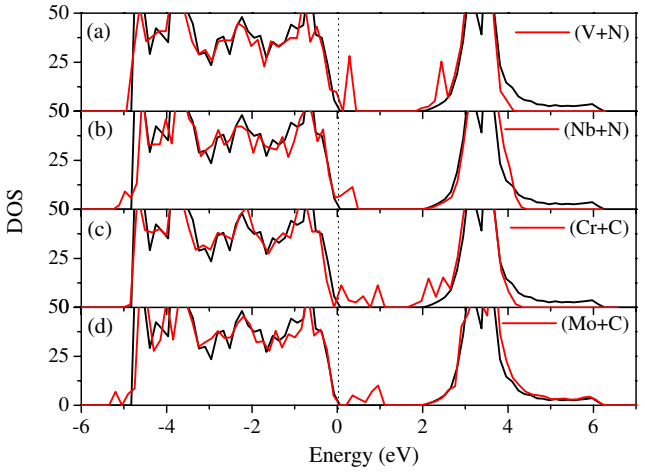

FIG. 4 (color online). The LDA-calculated DOS of undoped TiO_2 and (V + N), (Nb + N), (Cr + C), and (Mo + C)-codoped TiO_2. The Fermi level of pure TiO_2 is displayed with a dashed line.

TABLE I. The calculated ΔE_v, ΔE_c, and ΔE_g for anatase TiO_2 doped with different passivated impurity pairs. Positive number indicates an increase in energy with respect to pure TiO_2.

Systems	ΔE_v	ΔE_c	ΔE_g
TiO_2:(N + V)	0.38	−0.11	−0.49
TiO_2:(N + Nb)	0.42	0.05	−0.37
TiO_2:(C + Cr)	1.05	−0.31	−1.36
TiO_2:(C + Mo)	1.04	−0.08	−1.12

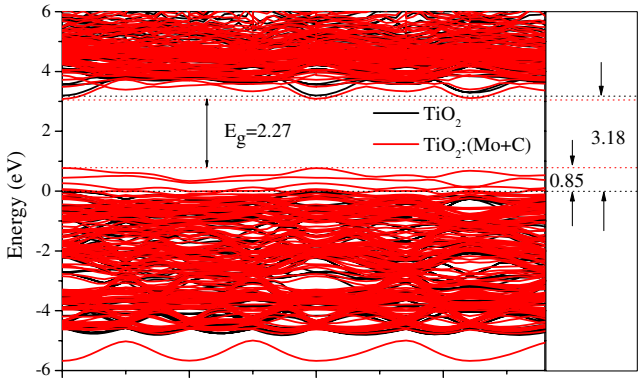

FIG. 5 (color online). The band structure comparison between pure TiO_2 and TiO_2:(Mo + C) calculated with LDA + U.

has the ability to keep its reducing power for hydrogen production under visible light. Furthermore, the formation of high-lying passivated defect valence band in TiO_2:(Mo + C) can also help overcoming the *p*-type doping difficulty in wide-band-gap semiconductors such as TiO_2 [22,23].

To verify that the conclusion of our calculation is not affected by the underestimated band gap in our LDA calculation, we have also performed LDA + U calculations for pure TiO_2 and TiO_2:(Mo + C), where the U parameters are fitted to the experimental band gap of TiO_2 (3.2 eV) and MoO_3 (2.1 eV) [24]. The calculated LDA + U band structures and band alignments between TiO_2 and TiO_2:(Mo + C) are displayed in Fig. 5. The obtained band gap for TiO_2:(Mo + C) is 2.26 eV, close to that predicted from LDA calculation (2.1 eV), indicating that the LDA band-gap error in systems with and without dopants is similar. The large dispersion at the top of the VBM also indicates that the C-derived defect bands are not too localized to limit the light absorption if the (Mo + C) concentration is reasonably large.

Binding energy of defect pairs.—To see if the formation of these defect pairs are stable, we calculated the defect pair binding energy [25] $E_b = E(\mathrm{Mo_{Ti}}) + E(\mathrm{C_O}) - E(\mathrm{Mo_{Ti}} + \mathrm{C_O}) - E(\mathrm{TiO_2})$, where E is the total energy of the system calculated with the same supercell. Positive E_b indicates that the defect pairs tend to bind to each other when both are present in the sample. The calculated binding energies E_b for the (V + N), (Nb + N), (Cr + C), and (Mo + C) pairs are 2.11, 1.97, 2.92, and 3.32 eV, respectively, indicating that the pairs are stable with respect to the isolated impurities. The large binding energy results from charge transfer from donor to acceptors and the associated strong Coulomb interaction between positively charged donors and negatively charged acceptors.

In summary, based on first-principles band structure calculations and analysis of the band-edge wave function characters, we propose that passivated (Mo + C)-doped TiO_2 is a strong candidate for PEC hydrogen production through water splitting, because it reduces the band gap to the ideal visible-light region, but does not affect much of the position of CBM. We suggest that the design principles discussed in this Letter can also be applied to other wide-band-gap semiconductors.

J. L. gratefully acknowledges financial support from "One-hundred Talent Plan" of the Chinese Academy of Sciences. This work is supported by the National Basic Research Program of China (973 Program) Grant No. G2009CB929300 and the National Natural Science Foundation of China under Grants No. 60521001 and No. 6077061. The work at NREL is supported by the U.S. DOE under Contract No. DE-AC36-08GO28308.

*jbli@semi.ac.cn
†swei@nrel.gov

[1] A. Fujishima and K. Honda, Nature (London) **238**, 37 (1972).
[2] M. Grazel, Nature (London) **414**, 338 (2001).
[3] S. Khan, J. M. Al-Shahry, and W. B. Ingler, Science **297**, 2243 (2002).
[4] M. R. Hoffmann, S. T. Martin, W. Y. Choi, and D. W. Bahnmann, Chem. Rev. **95**, 69 (1995).
[5] O. K. Khaselev and J. A. Turner, Science **280**, 425 (1998).
[6] R. Asahi, T. Morikawa, T. Ohwaki, K. Aoki, and Y. Taga, Science **293**, 269 (2001).
[7] G. R. Torres *et al.*, J. Phys. Chem. B **108**, 5995 (2004).
[8] T. Umebayashi, T. Yamaki, H. Itoh, and K. Asai, Appl. Phys. Lett. **81**, 454 (2002).
[9] J. L. Gole *et al.*, J. Phys. Chem. B **108**, 1230 (2004).
[10] H. Irie, Y. Watanabe, and K. Hashimoto, Chem. Lett. **32**, 772 (2003).
[11] T. Umebayashi, T. Yamaki, H. Itoh, and K. Asai, J. Phys. Chem. Solids **63**, 1909 (2002).
[12] J. M. Herrmann, J. Disdier, and P. Pichat, Chem. Phys. Lett. **108**, 618 (1984).
[13] W. Mu, J. M. Herrmann, and P. Pichat, Catal. Lett. **3**, 73 (1989).
[14] K.-S. Ahn, Y. Yan, S. Shet, T. Deutsch, J. Turner, and M. Al-Jassim, Appl. Phys. Lett. **91**, 231909 (2007).
[15] M. N. Huda, Y. Yan, S.-H. Wei, and M. Al-Jassim, **78**, 195204 (2008).
[16] P. E. Blöchl, **50**, 17953 (1994); G. Kresse and J. Joubert, **59**, 1758 (1999).
[17] G. Kresse and J. Hafner, **47**, 558 (1993); **48**, 13115 (1993).
[18] L. Kavan, M. Gräzel, S. E. Gilbert, C. Klemenz, and H. J. Scheel, J. Am. Chem. Soc. **118**, 6716 (1996).
[19] C. J. Howard, T. M. Sabine, and F. Dickson, Acta Crystallogr. Sect. B **47**, 462 (1991).
[20] H. J. Monkhorst and J. D. Pack, **16**, 1748 (1977).
[21] C. D. Valentin, G. Pacchioni, and A. Selloni, Chem. Mater. **17**, 6656 (2005).
[22] Y. Yan, J. Li, S.-H. Wei, and M. M. Al-Jassim, Phys. Rev. Lett. **98**, 135506 (2007).
[23] P. Ma *et al.*, Appl. Phys. Lett. **93**, 102112 (2008).
[24] R. Coquet and D. J. Willock, Phys. Chem. Chem. Phys. **7**, 3819 (2005).
[25] J. Li, S.-H. Wei, S. S. Li, and J. B. Xia, **74**, 081201 (2006).